10.24425/acs.2023.146957

Archives of Control Sciences
Volume 33(LXIX), 2023
No. 3, *pages 539–563*

Review, design, stabilization and synchronization of fractional-order energy resources demand-supply hyperchaotic systems using fractional-order PD-based feedback control scheme

Ammar SOUKKOU , Yassine SOUKKOU , Sofiane HADDAD ,
Mohamed BENGHANEM and Abdelhamid RABHI

This paper introduces a fractional-order PD approach (F-oPD) designed to control a large class of dynamical systems known as fractional-order chaotic systems (F-oCSs). The design process involves formulating an optimization problem to determine the parameters of the developed controller while satisfying the desired performance criteria. The stability of the control loop is initially assessed using the Lyapunov's direct method and the latest stability assumptions for fractional-order systems. Additionally, an optimization algorithm inspired by the flight skills and foraging behavior of hummingbirds, known as the Artificial Hummingbird Algorithm (AHA), is employed as a tool for optimization. To evaluate the effectiveness of the proposed design approach, the fractional-order energy resources demand-supply (Fo-ERDS) hyperchaotic system is utilized as an illustrative example.

Key words: fractional-order systems, fractional-order control, Lyapunov stability theory, multiobjective optimization, artificial hummingbird algorithm, stabilization and synchronization, energy resources demand-dupply systems.

A. Soukkou (corresponding author, e-mail: soukkou.amr@gmail.com) and S. Haddad are with Renewable Energy Laboratory, Faculty of Science and Technology, Department of Electronics, University of MSBY Jijel, BP. 98, Ouled Aissa, Jijel, Algeria.

Y. Soukkou is with Research Center in Industrial Technologies CRTI, P. O. Box. 64, Cheraga 16014, Algiers, Algeria.

M. Benghanem is with Physics Department, Faculty of Science, Islamic University of Madinah, Madinah, KSA.

A. Rabhi is with Modeling, Information and Systems Laboratory, University of Picardie Jules Verne, Amiens, France.

Received 4.10.2022. Revised 6.06.2023.

1. Introduction

Fractional-order calculus (F-oC) has been a subject of discussion in the field of applied mathematics for almost three centuries since its establishment. Over time, F-oC has proven to be an exceptionally powerful approach for characterizing the dynamics of physical systems and describing various physical phenomena [1–6]. In a series of studies [7–12], researchers utilized the fractional-order representation of electronic components and applied it to power systems. Furthermore, in [13] several examples were presented showcasing the adoption of F-oC in various industrial applications. These studies demonstrate the potential of fractional-order differential equations in providing more accurate representations of real-world systems. Consequently, fractional-order systems have gained significant attention in multidisciplinary areas such as physics, engineering, economics, control systems, and signal processing.

Various formulations of fractional-order operators have been extensively studied, including the Riemann-Liouville, Caputo, Caputo-Fabrizio, and Grünwald-Letnikov definitions [14, 15]. In [16], a comprehensive overview was presented, highlighting different approximation and discretization approaches used to estimate and evaluate fractional derivatives and integrals. The importance of developing sophisticated algorithms becomes evident as they provide convenient numerical tools for solving fractional-order differential equations [17–29]. For instance, a fourth-order fractional Runge-Kutta solver was proposed in [24]. Furthermore, the authors in [25] introduced a generalized form of Euler functions for solving differential equations with fractional-order.

Fractional-order chaotic systems (F-oCSs), which are extensions of ordinary chaotic systems, have captured the attention of numerous researchers as an alternative representation for studying and controlling chaotic behavior within this class of dynamical systems [5]. A comprehensive review of F-oCSs was provided by the author in [30]. In another study, Chen et al. [20] presented a systematic approach for designing various types of F-oCSs. The stabilization and synchronization of F-oCSs have been extensively investigated, employing advanced control techniques and artificial intelligence methods, owing to their significant relevance in real-world applications [5, 31].

The advancement of system dynamics modeling using fractional-order calculus (F-oC) has led to a significant interest in the hypothesis of utilizing fractional-order controllers by numerous researchers and applications [15,24,32,33]. Consequently, the concept of fractional-order control has been extensively investigated in both the stabilization and the synchronization processes of F-oCSs [34–41]. Combining the F-oC concept with prediction-based control, novel approaches for stabilizing and synchronizing a large class of F-oCSs were proposed by the authors in [36, 37]. The design process involved the utilization of Lyapunov stabilization assumptions and evolutionary algorithms. Soukkou et al. introduced an optimal fractional-order controller for controlling and synchronizing F-oCSs, based on BIBO stability assumptions, small gain hypothesis, and matrix norms concepts, as described in [38, 39]. Additionally, a time-delayed feedback control strategy in fractional form was proposed in [40] to stabilize and to synchronize a specific class of F-oCSs. However, developing controllers with high efficiency and low cost for nonlinear systems, particularly F-oCSs, remains a challenging task. Furthermore, several open issues persist in the fields of fractional-order modeling and control. These include the design of control laws, the discretization mechanism of fractional-order derivative and integral operators [14–20, 23–29, 42, 43], stability analysis [16, 44–48], and real-time implementation of fractional operators [49–54].

The present work emphasized fractional-order control based on state predictions for F-oCS, initially presented in [36–39, 55] with significant improvements. The aim is to strengthen performance by selecting the most appropriate analysis and synthesis tools for the system's nonlinearity and fractional representation. As a result, the ultimate purposes of this work revolve around flexibility of analysis and synthesis, and enhancement of system behavior. The fractional-order control strategy is used in this paper to establish the PD controller's fractional-order model to synchronize and to stabilize a class of F-oCSs. The proposed F-oPD approach with appropriate knowledge base is designed by using the multiobjective optimization algorithm with the guarantee of Lyapunov stability constraints of F-oCSs. Ultimately, numerical simulations are shown to affirm the feasibility of the proposed design, by taking the Fo-ERDS hyperchaotic system as such an illustrative example.

The structure of this paper is organized as follows: Section 2 provides an introduction to the fundamental concepts, properties, and theoretical background of F-oC and F-oCSs, which are relevant to the present study. In Section 3, a fractional-order control law specifically designed for stabilizing and synchronizing a class of F-oCSs is proposed and extensively examined. The optimization process is thoroughly explained in Section 4. Section 5 presents simulation results that demonstrate the effectiveness of the proposed approach. Finally, Section 6 concludes the paper, summarizing the main findings and contributions of the present work.

2. Preliminaries

Subsequently, we introduce several definitions and lemmas related to fractional calculus, which play a crucial role in this study.

Definition 1 *[14]: Given that ${}_{t_0}I_t^q x(t)$ represents the fractional-order integral of order $q \in \mathbb{R}^+$ in the case of a continuous function $x(t)$ which would be calculated* *by the following equation*

$$ {}_{t_0}I_t^q x(t) = {}_{t_0}D_t^{-q} x(t) = \frac{1}{\Gamma(q)} \int_{t_0}^{t} \frac{x(\tau)}{(t-\tau)^{1-q}} \mathrm{d}\tau, \quad t > t_0\,, \tag{1} $$

where t_0 *is the starting time.* $\Gamma(q)$ *is the Eulers Gamma function defined by* $\Gamma(\upsilon) \triangleq (\upsilon - 1)!$, *with its property* $\Gamma(\upsilon + 1) \triangleq \upsilon \cdot \Gamma(\upsilon)$.

Definition 2 *[22]: The definition of Grünwald-Letnikov (GL) is the most suitable for the numerical discretization of the fractional-order derivative operator. The GL derivative of continous function* $x(t)$ *can be approached as*

$$ {}_a^{\mathrm{GL}}D_t^q x(t) \cong \lim_{h \to 0} h^{-q} \sum_{i=0}^{M} c_i^q x(t - ih), \tag{2} $$

where $M = [(t - a)/h]$ *reflects the upper limit of the calculation horizon,* $[\cdot]$ *is the integer component, whereas* h *is the sample time.* c_i^q, $i \geqslant 0$ *defines the binomial coefficients computed using the following relationship*

$$ c_{i \geqslant 0}^q = (-1)^i \cdot \binom{q}{i} = \begin{cases} 1, & i = 0 \\ (1 - (1 + q)/i) \cdot c_{i-1}^q, & \forall i > 0. \end{cases} \tag{3} $$

Definition 3 *[14]: The Mittag-Leffler function with two parameters is the most commonly used. Its formula is given by*

$$ E_{\alpha,\beta}(\zeta) = \sum_{k=0}^{\infty} \zeta^k big/\Gamma(\alpha k - \beta), \tag{4} $$

where $\alpha > 0$, $\beta > 0$. *For* $\beta = 1$, *we have* $E_\alpha(\zeta) = E_{\alpha,1}(\zeta)$. *Also,* $E_{1,1}(\zeta) = e^\zeta$.

Lemma 1 *[14]: If* $\theta \in [\pi\alpha/2, \pi\alpha]$, *then there exists* $\Upsilon > 0$, *so that the Mittag-Leffler function is described by*

$$ E_{\alpha,\beta}(\zeta) \leqslant \Upsilon \big/ \left(1 + |\zeta|\right), \qquad \beta \leqslant |\arg(\zeta)| \leqslant \pi, \quad |\zeta| \geqslant 0. \tag{5} $$

2.1. Preliminaries of F-oCSs

The most used representation of the n-dimension controlled F-oCSs with order $q \in \mathbb{R}^+$without external disturbances is illustrated as follows

$$ {}_0D_t^q x(t) = Ax(t) + \psi\left(t, x(t)\right) + u\left(x(t)\right), \quad t > 0, \quad x(0) = x_0\,, \tag{6} $$

where $x(t) \in \mathbb{R}^n$ and $u(x(t)) = \widetilde{S}_w \Phi(x(t)) \in \mathbb{R}^n$ are the vector of states and the control signal, respectively. $\widetilde{S}_w \in \mathbb{R}^{n \times n}$ is a switch matrix in which $\widetilde{s}_{ij} = \{0, 1\}$ that indicates which of the state variables need to be controlled. The function $\psi(t, x(t)) \mapsto [0, \infty) \times \mathbb{R}^n \longrightarrow \mathbb{R}^n$ represents a continuous nonlinear function that fulfills the Lipschitz condition in regards to $x(t)$, and $x_0 \in \mathbb{R}^n$ is the initial condition. $A \in \mathbb{R}^{n \times n}$ is a matrix. We assume that $\psi(\cdot)$ is differentiable and the system (6) exhibits chaotic behavior when $\Phi(\cdot) = 0$ [34].

3. Problem formulation

Note that $x_j^* = \left(x_1^*, x_2^*, \cdots, x_n^*\right)^T$ represents either the j-th unstable equilibrium point (case of stabilization process (Stab_P)) or the outputs of the master F-oCS (case of synchronization process (Sync_P)). The mathematical formulation can be represented according to the type of operation related to the system under control, as

$$\text{Stab\_P:} \qquad \begin{cases} x_j^* = \left(x_{1j}^*,\, x_{2j}^*,\, \cdots,\, x_{nj}^*\right), \\ D_t^{q_s} y(t) = f\,(t, y(t)) + \widetilde{S}_w \Phi(x, y), \end{cases} \tag{7}$$

$$\text{Sync\_P:} \qquad \begin{cases} \text{(M)} \mapsto D_t^{q_m} x(t) = f\,(t, x(t))\,, \quad x(0) = x_0\,, \\ \text{(S)} \mapsto D_t^{q_s} y(t) = g\,(t, y(t)) + \widetilde{S}_w \Phi(x, y), \quad y(0) = y_0\,, \end{cases} \tag{8}$$

where $x(t) \in \mathbb{R}^n$ and $y(t) \in \mathbb{R}^n$ are the states of master (M) and salve (S) systems, respectively. $f(t, x(t)) : \mathbb{R}^n \mapsto \mathbb{R}^n$ and $g(t, y(t))$ representing their nonlinearities. $\Phi(\cdot) \in \mathbb{R}^n$ is the control law to be adopted. The main objective is to establish an appropriate control law such that the trajectory of the dynamical process (S) will be asymptotically approaches that of the reference signal generator (M). The general model describing all of the possibilities relevant to both stabilizing and synchronizing the F-oCSs will be summarized as follows

$$\lim_{t \mapsto \infty} \|e(t)\|_i = \lim_{t \mapsto \infty} \|y(t) - x(t)\|_i \mapsto 0, \quad i = 1, 2, \infty. \tag{9}$$

It's noted that the control outputs must be thresholded and $f(\cdot)$ fulfills the Lipschitz condition such that for any $v(t) \in \mathbb{R}^n$, and for the Lipschitz constant $\varepsilon > 0$

$$\|f\,(v(t))\|_i \leqslant \varepsilon\,\|v(t)\|_i\,, \quad t \in \mathbb{R}^+, \;\; i = 1, 2, \infty. \tag{10}$$

Property 1 *When the state variables approach their references, the stabilization as well as the synchronization process is started, i.e,*

$$u(t) = \begin{cases} \widetilde{S}_w \Phi(x, y) & \textit{if} \;\; |y - x| < \xi, \\ 0, & \textit{otherwise}, \end{cases} \tag{11}$$

where $\xi \geqslant 0$ *is a given adequately smaller positive number.*

3.1. Descretization of fractional-order PD controller

Next, we consider the simplified form of F-oPD control strategy to stabilize and to synchronize a class of F-oCSs. If the constraints imposed by Eq. (11) are satisfied, then it is useful to design a controller $\Phi(\cdot)$ such that the corresponding state variable $x(t)$ of system (6) needs to satisfy (9). The control signal is established by

$$\Phi(t) = \widetilde{\mathrm{K}}_{\mathrm{D}} D_t^q \widetilde{x}(t) + \widetilde{\mathrm{K}}_{\mathrm{P}} \widetilde{x}(t), \qquad q \in \mathbb{R}^+, \quad t > 0, \tag{12}$$

where $\widetilde{x}(t) = y(t) - x(t)$ is the tracking error, $\widetilde{\mathrm{K}}_{\mathrm{P}} \in \mathbb{R}^{n\times n}$ and $\widetilde{\mathrm{K}}_{\mathrm{D}} \in \mathbb{R}^{n\times n}$ are the control matrices to be determined. Taking $t \mapsto t_k = k \cdot h$, $\widetilde{x}^j(t_k) \mapsto \widetilde{x}^j_k$ and $\Phi^j(t_k) \mapsto \Phi^j$, the j-th control law ($j = 1, 2, \ldots$) can be formulated by using the GL definition 2, as

$$\begin{aligned} \Phi^j = {} & \left(\widetilde{\mathrm{K}}^j_{\mathrm{P}} + \widetilde{\mathrm{K}}^j_{\mathrm{D}} h^{-q_j} c^j_0\right) \widetilde{x}^j_k - \left(-\widetilde{\mathrm{K}}^j_{\mathrm{D}} h^{-q_j} c^j_1\right) \widetilde{x}^j_{k-1} \\ & + \widetilde{\mathrm{K}}^j_{\mathrm{P}} h^{-q_j} \left[c^j_2 \widetilde{x}^j_{k-2} - \left(-c^j_3\right) \widetilde{x}^j_{k-3} \right] + \cdots \end{aligned} \tag{13}$$

According to Eq. (13), an unlimited filter is not physically realizable. As a consequence, it is necessary to establish an approximation approach in appropriate windows of length N that is perfectly suited for physical implementation. The discrete F-oPD equation can be rewritten in approached and generalized form by rearranging the previous equation (13), as

$$\begin{gathered} \Phi^j \cong \widetilde{\Phi}^j_{\mathrm{PD}_0} + \sum_{i=1}^{N} \Phi^j_{\mathrm{PD}_i}, \\ \begin{cases} \widetilde{\Phi}^j_{\mathrm{PD}_0} = \widetilde{\Psi}^j_0 \cdot \widetilde{x}^j_k + \Psi^j_1 \cdot \widetilde{x}^j_{k-1}, \\ \Phi^j_{\mathrm{PD}_i} = \Psi^j_{2i} \cdot \widetilde{x}^j_{k-2i} + \Psi^j_{2i+1} \cdot \widetilde{x}^j_{k-(2i+1)}, \quad i = 1, 2, \ldots, \end{cases} \end{gathered} \tag{14}$$

where $\widetilde{\Psi}^j_0 = \widetilde{\mathrm{K}}^j_{\mathrm{P}} + \Psi^j_0$ and $\Psi^j_l = \widetilde{\mathrm{K}}^j_{\mathrm{D}} h^{-q_j} \cdot c^j_l$, $(l = 2, 3, \cdots, N)$. If $N = 0$, then Eq. (14) is equivalent to integer-order control strategy. In other words, Eq. (14) may be seen as an interconnected PD processing unit having $(N+1)$ nodes (regulators) temporarily shifted. From Eq. (14), each iteration involves a re-calculation and even a summation of every earlier time level $\sum_{i=v}^{n}\Psi_i^j\cdot\widetilde{x}_{k-i}^j$. For the memory context represented as a sum, the 'principle of short memory' established by Podlubny in the well-known work [14] should be implemented, where the data is stored in the $[t-L,\ t]$ interval, in which L represents the memory length. If $|x(t)|\leqslant M, 0<t\leqslant t_1$, we can easily establish the following estimation, which provides adequate accuracy ξ_d, to determine the length of memory L [14].

$$L\geqslant\left(M_{em}/\xi_d\cdot|\Gamma(1-q)|\right)^{1/\widetilde{q}},\qquad \widetilde{q}=\max\left(q_{i=1,2,\cdots,n}\right). \tag{15}$$

Therefore, the dimensioning problem of the developed F-oPD approach can be considered as an optimization process. It can be pronounced as

$$\min_{\xi_d,M_{em},h}\left(\mathrm{tr}(N)\right). \tag{16}$$

Subject to

$$\begin{cases}\displaystyle\sum_{k=0}^{l-1}\widetilde{x}^T(k)P_x\widetilde{x}(k)\leqslant\xi_d^T, \quad P_x=\widetilde{q}\mathrm{I}_{m\times m},\ \ \widetilde{q}\in\mathbb{R},\\ L\geqslant\left(M_{em}/\xi_d\,|\Gamma(1-q)|\right)^{1/\widetilde{q}},\quad \widetilde{q}=\max\left(q_{i=1,2,\cdots,n}\right).\end{cases} \tag{17}$$

3.2. F-oPD scheme for stabilizing F-oCSs

In this part of the paper, we will develop F-oPD control law to stabilize the F-oCSs around the equilibrium point (EPs) x^*, *i.e.*, $\widetilde{x}(t)=x^*-x(t)$. Taking into consideration the control law (12), the new formulation of (6) with $D_t^q x^*=0$ can be rewritten as

$$D_t^q x(t)=\mathfrak{A}x(t)+\widetilde{\psi}_s\left(t,x(t)\right)+\widetilde{\mu}, \tag{18}$$

where $\widetilde{\mathfrak{A}}=A-\widetilde{S}_w\left(\widetilde{\mathrm{K}}_\mathrm{P}+\widetilde{\mathrm{K}}_\mathrm{D}A\right)$, $\widetilde{\Upsilon}=\left(\mathrm{I}-\widetilde{S}_w\widetilde{\mathrm{K}}_\mathrm{D}\right)$, $\widetilde{\psi}_s(t,x(t))=\widetilde{\Upsilon}\psi(t,x(t))$ and $\widetilde{\mu}=\widetilde{S}_w\widetilde{\mathrm{K}}_\mathrm{P}x^*$.

Theorem 1 *Let $x=x^*$ the EP of the uncontrolled F-oCS (6) with $\Phi(\cdot)=0$. Assume there exist a matrix $P=P^T>0$ as well as a knowledge base*

$$\Lambda_{\mathrm{KB}}=\left\{\overbrace{\underbrace{\left(\widetilde{\mathrm{K}}_\mathrm{P},\ \widetilde{\mathrm{K}}_\mathrm{D}\right)}_{\in\mathbb{R}^{n\times n}}}^{Control\ parameters},\ \overbrace{\underbrace{\widetilde{S}_w}_{\substack{\in\{0,1\}\\ Activation}},\ \underbrace{\underbrace{N_1,\ \ldots,\ N_n,}_{\in\mathbb{N}}}_{Dimension}\ \underbrace{\underbrace{q_j}_{j=1,\cdots,n},\ \underbrace{H}_{\in\mathbb{R}^{n\times n}}}_{Order/Sample}}^{Structural\ parameters}\right\}, \tag{19}$$

satifies the inequality

$$\lambda_{\min}(Q) > \varepsilon \cdot \|P\|_i \cdot \left\|\widetilde{\Upsilon}\right\|_i + \frac{1}{2}, \qquad \varepsilon > 0, \quad i = 1, 2, \infty. \tag{20}$$

Then, the nonlinear controlled F-oCS (6) is asymptotically stable, where $Q = P\widetilde{\mathfrak{A}}$.

Proof. Before illustrating the previous Theorem, below, some Lemmas are presented and used for the study of stability in the Lyapunov sense.

Lemma 2 *[56] For a specified derivable and continuous function* $\varphi(t) \in \mathbb{R}^n$, *and* $\widetilde{P} = \widetilde{P}^T > 0$, *the Caputo's derivative operator fulfills the following expression*

$$\frac{1}{2}{}^{\mathrm{C}}_{t_0}D^{\alpha}_{t}\left(\varphi^T(t)\widetilde{P}\varphi(t)\right) \leqslant \varphi^T(t)\widetilde{P}{}^{\mathrm{C}}_{t_0}D^{\alpha}_{t}\varphi(t); \ \ \forall\, 0 < \alpha < 1, \ \ \forall\, t \geqslant t_0 \geqslant 0. \tag{21}$$

Lemma 3 *[57] If such a Lyapunov function* $V\colon \mathbb{R}^n \to \mathbb{R}^n$ *as well as a class-K function* $\partial_{l=1\sim 3}$ *exist, satisfied the following inequalities, as*

$$\partial_1\left(\|x(t)\|_{i=1,2,\infty}\right) \leqslant V\left(t, x(t)\right) \leqslant \partial_2\left(\|x(t)\|_{i=1,2,\infty}\right), \tag{22}$$

$$D^{\beta}_{t}V\left(t, x(t)\right) \leqslant -\partial_3\left(\|x(t)\|_{i=1,2,\infty}\right), \quad 0 < \beta \leqslant 1. \tag{23}$$

The system (6) is then asymptotically stable ($\lim_{x\mapsto\infty} x(t) = x^*$).

Lemma 4 *For a continuous function* $\wp(x(t)) = x^T(t)\widetilde{\mathrm{A}}x(t)$, *if a positive definite matrix* $\widetilde{\mathrm{A}}$ *exists, then*

$$\lambda_{\min}\left(\widetilde{\mathrm{A}}\right)\|x(t)\|^2_{i=1,2,\infty} \leqslant \wp\left(x(t)\right) \leqslant \lambda_{\max}\left(\widetilde{\mathrm{A}}\right)\|x(t)\|^2_{i=1,2,\infty}, \tag{24}$$

where $\lambda_{\min}\left(\widetilde{\mathrm{A}}\right)$ *and* $\lambda_{\max}\left(\widetilde{\mathrm{A}}\right)$ *represent the minimum and maximum eigenvalues of the matrix* $\widetilde{\mathrm{A}}$, *respectively.*

According to Lyapunov's theory and by analogy with systems of integer-order, we have the stability for any initial condition if there exists a function $V(x)$ such that for $x \neq 0$, $V(x) > 0$ and $D^q_t V(x) < 0$. Let $P = P^T \in \mathbb{R}^{n\times n}$ a positive definite matrix to be determined. We assume given a Lyapunov candidate function for the system described by

$$V(x(t)) = x^T(t)Px(t). \tag{25}$$

For any initial state vector of the nonlinear controlled F-oCS, it would be useful to demonstrate that $D^q_t V < 0$ (**Step 1**) and V in (25) tends to decrease and $x(t)$ converges towards the origin (**Step 2**).

- **Step 1:** By using Lemma 2, $D_t^q V(x(t))$ will be evaluated as follows

$$D_t^q V(x(t)) \leqslant -2x^T(t)Qx(t) + 2x^T(t)P\widetilde{\Upsilon}\psi(t, x(t)) + 2x^T(t)P\widetilde{\mu}, \tag{26}$$

where $Q = P\widetilde{\mathfrak{A}}$. By using Lemma 4 and applying the Lipschitz continuous property of $\psi(t, x(t))$ and $Q = Q^T > 0$, $D_t^q V$ becomes

$$\begin{aligned} D_t^q V(x(t)) &\leqslant -2\lambda_{\min}(Q)\,\|x(t)\|_i^2 + 2\varepsilon x^T(t)P\widetilde{\Upsilon}\,\|x(t)\|_i + 2x^T(t)P\widetilde{\mu} \\ &\leqslant -2\lambda_{\min}(Q)\,\|x(t)\|_i^2 + 2\varepsilon\,\|P\|_i \left\|\widetilde{\Upsilon}\right\|_i \|x(t)\|_i^2 \\ &\quad + 2\cdot x^T(t)\cdot P\cdot\widetilde{\mu}, \quad i = 1, 2, \infty. \end{aligned} \tag{27}$$

According to Young's inequality, the following expression appears to be true.

$$x^T(t)P\widetilde{\mu} \leqslant \frac{1}{2}\|x(t)\|_i^2 + \frac{1}{2}\|P\widetilde{\mu}\|_i^2, \quad i = 1, 2, \infty. \tag{28}$$

Based on Eq. (24) in Lemma 4 and for $0 < \|x(t)\|_i < \delta$, $D_t^q V$ becomes

$$D_t^q V(x(t)) \leqslant -\left(\left(2\lambda_{\min}(Q) - 2\varepsilon\|P\|_i\left\|\widetilde{\Upsilon}\right\|_i - 1\right)\Big/\lambda_{\max}(P)\right)V(x(t)) + \|P\widetilde{\mu}\|_i^2, \quad i = 1, 2, \infty,$$

where $\lambda_{\max}(P)$ denotes the maximum eigenvalue of the matrix P which is positive. Select $\varepsilon < 0.5(2\lambda_{\min}(Q) - 1)/\|P\|_i\left\|\widetilde{\Upsilon}\right\|_i$, ensure that

$$D_t^q V(x(t)) \leqslant -\widetilde{\phi}V(x(t)) + \widetilde{\varphi}, \tag{29}$$

where $\widetilde{\phi} = 2\left(\lambda_{\min}(Q) - \varepsilon\|P\|_i\left\|\widetilde{\Upsilon}\right\|_i - \frac{1}{2}\right)\Big/\lambda_{\max}(P)$ and $\widetilde{\varphi} = \|P\cdot\widetilde{\mu}\|_i^2$, $i = 1, 2, \infty$.

Since $V > 0$ in Eq. (25) and in ordre to guaranty the asymptotic stability condition of the controlled system (18), it is necessary that $D_t^q V < 0$ in Eq. (29) satisfies

$$\|P\widetilde{\mu}\|_i^2\,\lambda_{\max}(P)\Big/\left(2\lambda_{\min}(Q) - 2\varepsilon\|P\|_i\left\|\widetilde{\Upsilon}\right\|_i - 1\right) > 0, \quad i = 1, 2, \infty. \tag{30}$$

From Eq. (30), it can be remarked that $\|P\widetilde{\mu}\|_i^2 > 0$ and $\lambda_{\max}(P) > 0$. In order to satisfy the condition (30), it is necessary that

$$\lambda_{\min}(Q) > \varepsilon\|P\|_i\left\|\widetilde{\Upsilon}\right\|_i + 0.5, \quad i = 1, 2, \infty. \tag{31}$$

The inequalities (30) and (31) establish the closed-loop system's stability. Moreover, the controlled F-oCS is asymptotically stable at the EP x^*. The proof of Theorem 1 is complete. □

- **Step 2:** Equation (29) can be rewritten as follows

$$D_t^q V\left(x(t)\right) - \widetilde{\varphi} \leqslant -\widetilde{\phi} V\left(x(t)\right). \tag{32}$$

By applying the Laplace transform, we get

$$s^q V(s) - V(0)s^{q-1} - \widetilde{\varphi}(s) \leqslant -\widetilde{\phi} V(s).$$

Which implies that

$$V(s) \leqslant \frac{V(0)s^{q-1} + \widetilde{\varphi}(s)}{s^q + \widetilde{\phi}} \leqslant V(0)\frac{s^{q-1}}{s^q + \widetilde{\phi}} + \frac{\widetilde{\varphi}(s)}{s^q + \widetilde{\phi}}, \tag{33}$$

where $V(0) = V(x(0))$. If $x(0) = 0 \Rightarrow V(0) = 0$ and $x = 0$ is the solution of the uncontrolled F-oCS (6).

Since, the Laplace transform of Mittag-Leffler function in two parameters (4) is given by [14]

$$Ł\left\{t^{\beta-1} E_{\alpha,\beta}\left(-\lambda t^{\alpha}\right)\right\} = s^{\alpha-\beta}/s^{\alpha} + \lambda, \quad t \geqslant 0.$$

In our particular case $\{\alpha, \beta\} = \{q, 1\}$ and $\lambda = \widetilde{\phi}$. In the event that $x(0) \neq 0 \Rightarrow V(0) > 0$ and the inverse Laplace transform of Eq. (33) will be obtained as follows

$$V(t) \leqslant V(0)E_q\left(-\widetilde{\phi}t^q\right) + \widetilde{\varphi}(t) * \left[t^{q-1}E_{q,q}\left(-\widetilde{\phi}t^q\right)\right], \tag{34}$$

where $*$ represents the operator for convolution. Since $t^{q-1} \geqslant 0$, $\forall q \in [0, 1]$ and $E_{q,q}\left(-\widetilde{\phi}t^q\right) \geqslant 0$, the second term of Eq. (34) can be ignored, which implies

$$V(t) \leqslant V(0)E_q\left(-\widetilde{\phi}t^q\right). \tag{35}$$

Since $P > 0$,

$$\begin{cases} \lambda_{\min}(P)\left\|x(t)\right\|_i^2 \leqslant V(t) = x^T P x \leqslant \lambda_{\max}(P)\left\|x(t)\right\|_i^2, \\ V(0) \geqslant \lambda_{\min}(P)\left\|x(0)\right\|_i^2, \quad i = 1, 2, \infty. \end{cases} \tag{36}$$

This implies as well that

$$\lambda_{\max}(P)\left\|x(t)\right\|_i^2 \leqslant V(0)E_q\left(-\widetilde{\phi}t^q\right), \quad i = 1, 2, \infty.$$

Consequently,

$$\left\|x(t)\right\|_i \cong \sqrt{\lambda_{\min}(P)/\lambda_{\max}(P)}\left\|x(0)\right\|_i E_q\left(\left(-\widetilde{\phi}t^q\right)\right)^{0.5}, \quad i = 1, 2, \infty. \tag{37}$$

By using Lemma 1, we have

$$\|x(t)\|_i \cong \sqrt{\lambda_{\max}(P)^{-1}\lambda_{\min}(P)}\|x(0)\|_i \left(1\Big/\left(1+\left\|-\widetilde{\phi}t^q\right\|_i\right)\right)^{0.5}, \quad i = 1, 2, \infty. \tag{38}$$

As a result, $\lim_{t\to\infty} x(t) = 0$ which implies that the controlled F-oCS (6) is asymptotically stable.

3.3. F-oPD scheme for synchronizing identical F-oCSs

Take into account the q-order identical fractional-order master (M) and slave (S) systems, characterised by

$$(\text{M}):\quad D_t^q x(t) = Ax(t) + f\left(x(t)\right), \qquad x(0) = x_0\,, \quad t \geqslant 0, \tag{39}$$

$$(\text{S}):\quad D_t^q y(t) = Ay(t) + g\left(y(t)\right) + \widetilde{\text{S}}_w\Phi(x, y), \qquad y(0) = y_0\,, \quad t \geqslant 0. \tag{40}$$

As previously stated, the objective is to establish an appropriate control law $\Phi(\cdot)$ that guarantees the slave system's trajectory (40) must follow the master system's trajectory (39) and, ultimately, achieves synchronization condition (9).

The error dynamics will be given as

$$\begin{aligned} D_t^q e(t) &= D_t^q y(t) - D_t^q x(t) \\ &= Ae(t) + \left(g\left(y(t)\right) - f\left(x(t)\right)\right) + \widetilde{S}_w\Phi\left(x, y\right). \end{aligned} \tag{41}$$

By replacing the model of the control law (12) in Eq. (41), the error dynamics (41) becomes

$$D_t^q e(t) = \widetilde{\mathfrak{A}}_e e(t) + \widetilde{\text{M}} f_{ms}\left(x(t), y(t)\right), \tag{42}$$

where $\widetilde{\mathfrak{A}}_e = A + \widetilde{S}_w\left(\widetilde{\text{K}}_\text{P} + \widetilde{\text{K}}_\text{D}A\right)$, $\widetilde{\text{M}} = \left(\text{I} + \widetilde{S}_w\widetilde{\text{K}}_\text{D}\right)$ and $f_{ms}(x(t), y(t)) = (g(y(t)) - f(x(t)))$.

Theorem 2 *Consider the F-oCSs (39) and (40). The synchronization process is established if and only if a positive definite matrix $P = P^T \in \mathbb{R}^{n\times n}$ and a knowledge base (19) exist, such that*

$$\widetilde{\lambda}_{\min}(Q_e) - \mu\widetilde{\lambda}_{\min}\left(\widetilde{Q}_{pm}\right) > 0, \tag{43}$$

where $Q_e = P\widetilde{\mathfrak{A}}_e$ and $\widetilde{Q}_{pm} = P \cdot \widetilde{\text{M}}$. Furthermore, the controlled slave F-oCS is asymptotically stable.

Proof. Let $P = P^T \in \mathbb{R}^{n\times n}$ to be positive definite matrix. We assume given a Lyapunov candidate function $V(e(t)) = e^T(t)Pe(t)$ for the system (42) and by using the same properties and techniques exploited in the stabilization process (previous section), $D_t^q V(e(t))$ will be evaluated as follows

$$D_t^q V(e(t)) \leqslant -\widetilde{\phi}_{xy} V(e(t)), \tag{44}$$

where $\widetilde{\phi}_{xy} = \left(\widetilde{\lambda}_{\min}(Q_e) - \varepsilon\widetilde{\lambda}_{\min}\left(\widetilde{Q}_{pm}\right)\right)/\widetilde{\lambda}_{\max}(P)$. In accordance with the direct Lyapunov method, $V(\cdot) > 0$ and $D_t^q V(\cdot) < 0$ in Eq. (44) are the two stability conditions for the controlled system (42). This implies that,

$$\widetilde{\lambda}_{\min}(Q_e) - \varepsilon\widetilde{\lambda}_{\min}\left(\widetilde{Q}_{pm}\right) > 0. \tag{45}$$

Expressions (44) and (45) guarantee stability in the sense of Lyapunov. Moreover, the two F-oCSs (39) and (40) are synchronized. The proof is complete. □

It is possible to convert the inequality (45) into an equality by adding a function $\gamma(t)$ such that

$$D_t^q V(e(t)) + \gamma(t) = -\widetilde{\phi}_{xy} V(e(t)). \tag{46}$$

Applying the Laplace transformation of Eq. (46) and with similarity of stabilization process (previous section), we have

$$\|e(t)\|_i \cong \sqrt{\lambda_{\max}(P)^{-1}\lambda_{\min}(P)}\|e(0)\|_i \left(1\Big/\left(1 + \left\|-\widetilde{\phi}_{xy}t^q\right\|_1\right)\right)^{0.5}, \quad i = 1, 2, \infty. \tag{47}$$

So that, $\lim_{t\to\infty} e(t) = 0$. This means that the system (42) is asymptotically stable.

4. Optimization strategy of the proposed F-oPD controller

In this study, we employ a bio-inspired optimization technique called the Artificial Hummingbird Algorithm (AHA) for finding the optimal parameters of the knowledge base (19) of the F-oPD controller. AHA is chosen for its ease of implementation and draws inspiration from hummingbird flight skills and foraging behavioral patterns.

4.1. Artificial Hummingbird Algorithm

The AHA is a recently developed optimization approach that draws inspiration from the foraging and flight behavior of hummingbirds. A detailed description of the basic algorithm can be found in [58]. The AHA algorithm is structured around four fundamental operations: initialization, guided foraging, territorial foraging, and migration foraging. Algorithm 1 describes the general structure of AHA.

Algorithm 1: General structure of AHA	
1:	Initialization () ;
2:	**While stop criterion is not satisfied do**
3:	Guided foraging () ;
4:	Territorial foraging () ;
5:	Migration foraging () ;
6:	**End;**

Designers who wish to create an optimization algorithm based on AHA should follow these four main steps:

1. Set the initial AHA configuration.
2. Establish a procedure for generating the initial population.
3. Determine the objective function that will be optimized.
4. Define the evolution process of AHA operators, specifically how to apply the basic operators of the algorithm: guided foraging, territorial foraging, and migration foraging.

Steps 2 to 4 are repeated until the optimization technique's stopping criterion, typically a predetermined number of iterations, is satisfied.

4.2. Optimization process

AHA can be applied to determine the most appropriate knowledge base (19), minimizing the objectives J_i, $(i = 1\sim n)$ while having to meet the design constraints g_i, $(i = 1\sim m)$. In our case, the multiobjective optimization problem can be formulated as follows

$$
\begin{aligned}
&\mathit{Minimize}\ \ J_i\,, \quad (i = 1, \cdots, 4) \\
&\begin{cases}
J_1 = N^{-1} \sum\limits_{k=0}^{N-1} \widetilde{x}^T(k)\widetilde{P}_x\widetilde{x}(k); & J_2 = N^{-1} \sum\limits_{k=0}^{N-1} u^T(k)\widetilde{Q}_x u(k); \\
J_3 = n^{-1} \sum\limits_{i=1}^{n} \widetilde{s}_{w_i}\,; & J_4 = \mathrm{tr}\,(\mathrm{N})\,;
\end{cases}
\end{aligned}
\tag{48}
$$

Subject to

$$\begin{cases} g_1 \mapsto \text{Eq. (17)} \\ g_2 \mapsto \begin{cases} \text{Eq. (20)}: & \text{Stab\_P} \\ \text{Eq. (43)}: & \text{Sync\_P} \end{cases} \\ \Lambda_{\text{KB}_{\min}} \leqslant \Lambda_{\text{KB}} \leqslant \Lambda_{\text{KB}_{\max}} \end{cases} \tag{49}$$

where $\widetilde{P}_x = \widetilde{q} \cdot \mathrm{I}_{n\times n}$ and $\widetilde{Q}_x = \widetilde{q} \cdot \mathrm{I}_{m\times m}$. $\Lambda_{\text{KB}_{\min}}$ and $\Lambda_{\text{KB}_{\max}}$ are the bounds of the parameters to be optimized Λ_{KB} (19). The constrained problem (48)–(49) is converted into an unconstrained problem by adopting the Exterior Penalty Function method described in [59].

In the next section, the Fo-ERDS hyperchaotic system is studied and analysed, given the context of energy resource demand in China's eastern regions and energy resource supply in China's western region.

5. System description

The chaotic and hyperchaotic ERDS systems have been introduced by Sun et al. [60, 61]. Otherwise, the fractional-order form of the three-dimensional ERDS system has been studied by authors in [40, 62, 63]. This section discusses the fractional-order form of the four-dimensional ERDS. The mathematical model of Fo-ERDS hyperchaotic system with orders $0 < q_i < 1$ $(i = 1{\sim}4)$ is dercribed by

$$\begin{aligned} D_t^{q_1} x &= a_1 x - a_2 y - a_2 z - d_3 w - a_1 x^2/M + s_{w1}\Phi_1(x, y, z, w), \\ D_t^{q_2} y &= b_3 N x - b_1 y - b_2 z - b_3 x(x - z) + s_{w2}\Phi_2(x, y, z, w), \\ D_t^{q_3} z &= -c_1 c_3 z + c_1 c_2 x z + s_{w3}\Phi_3(x, y, z, w), \\ D_t^{q_4} w &= d_1 x - d_2 w + s_{w4}\Phi_4(x, y, z, w), \end{aligned} \tag{50}$$

where x, y, z and w are the states of the system. The system parameters are extracted from references [60, 61]. More details about the parameters and variables characterizing the Fo-ERDS hyperchaotic system (50) are described in the references [60, 61]. In adition, the Fo-ERDS hyperchaotic system (50) admitted three unstable EPs of which the origin is a part while applying the theorems developed in [34]. For the numerical simulation of the behavior of the system, the GL method is used as a tool for discretizing fractional-order derivative operators with a sampling period $h = 0.01$ seconds. The commensurate Fo-ERDS hyperchaotic system with orders $q_{1\sim4} = 0.98$ under initial conditions (0.82, 0.29, 0.48, 0.1) g enerates chaotic behavior known as energy resource attractor, illustrated in Figure 1.

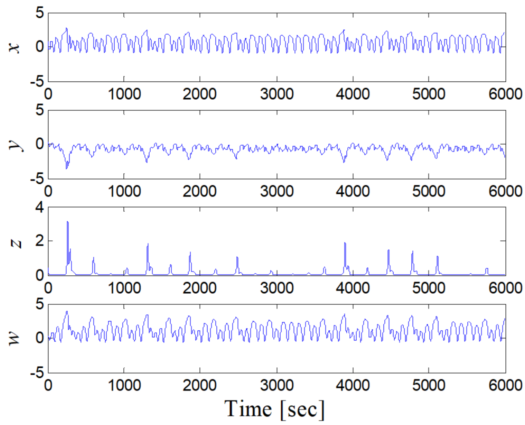

Figure 1: Simulation of the Fo-ERDS hyperchaotic system

5.1. Stabilizing of the Fo-ERDS hyperchaotic system

To verify the utility and efficiency of the proposed approach, we are interested throughout the system's stabilization around the unstable EP represented by the origin S_0. To simplify the design process, we propose using only the developed control law $u_1(t)$, and the remaining control laws are assumed to be null $u_i(t) = 0$, $(i = 2, 3, 4)$. In addition, we put $P = \widetilde{q}.\mathrm{I}$ with $\widetilde{q} = \sum_{i=1}^{n} q_i$. At the end of the execution of the optimization algorithm during 100 iterations, a feasible knowledge base is obtained: $\Lambda_{\mathrm{KB}} = \{(0.472, 0.446), (1, 0, 0, 0), 7, 0.98, 0.01\}$. When the F-oPD control law is applied at $t \geqslant 8.57$ [sec] as for $\zeta = 0.01$ (Condition (11) fulfilled), perfect stabilization of the EP S_0 is established in a short time as shown in Figure 2a which describes the evolution of system states.

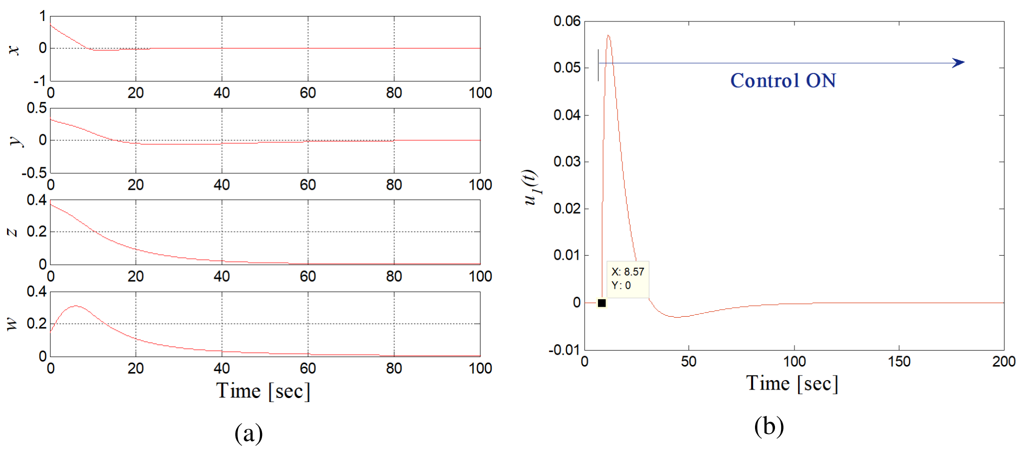

Figure 2: System states evolution (a) and the output of the control law (b)

In addition, the assumptions in Theorem 1 are achieved. It can be remarked that the F-oPD scheme presents the ability to achieve convergence towards the origin with relatively short transient responses. Additionally, Figure 2b represents the corresponding input signal.

To affirm the effectiveness of the designed algorithm, a comparative study between fractional-order with order $q_{1\sim 4} = 0.98$ and the integer-order PD (I-oPD) with order $q_{1\sim 4} = 1$ control laws (with reduced and full control inputs) is performed using the same AHA optimization procedure. Table 1 expresses the obtained results considering multiple performance factors.

Table 1: F-oPD and I-oPD controllers' performances

Design requirement	Type / Values			
Controller-type	F-oPD approach		I-oPD controller	
Active controller	$u_1(t)$	$u_i(t),\ \forall i$	$u_1(t)$	$u_i(t),\ \forall i$
Number of elementary controllers	$1^0_{\text{PD}} + 7$	$1^0_{\text{PD}} + 7$	1^0_{PD}	1^0_{PD}
		$1^0_{\text{PD}} + 3$		
		$1^0_{\text{PD}} + 2$		
		$1^0_{\text{PD}} + 6$		
IAE	1.09e+003	585.2493	2.07e+003	1.10e+003
ITAE	1.9287e+004	2.8094e+003	3.39e+004	4.85e+003
Chatering	/	/	++	+
Mataining time	~ 50 [sec]	~ 30 [sec]	~ 160 [sec]	~ 100 [sec]
Energy consumption $\sum_i \lvert u_i \rvert$	34.2642	35.9280	68.0816	70.9392
Controller complexity level	Medium	High	Low	Low
Number of parameters to be optimized	Medium	High	Low	Low

It can be noted that the controllers are activated even when the controlled Fo-ERDS hyperchaotic system approaches the origin. Furthermore, the controlled system has been found to be asymptotically stable.

5.2. Synchronization of Fo-ERDS hyperchaotic systems

To test the synchronization process between two identical commensurate Fo-ERDS hyperchaotic systems, we introduce a master (M)-slave (S) configuration with order $q_{i=1\sim4} = 0.98$ as

$$(\mathrm{M}): \quad \begin{cases} D_t^{q_1} x_m = a_1 x_m - a_2 y_m - a_2 z_m - d_3 w_m - a_1 x_m^2/M, \\ D_t^{q_2} y_m = b_3 N x_m - b_1 y_m - b_2 z_m - b_3 x_m (x_m - z_m), \\ D_t^{q_3} z_m = -c_1 c_3 z_m + c_1 c_2 x_m z_m, \\ D_t^{q_4} w_m = d_1 x_m - d_2 w_m, \end{cases} \tag{51}$$

$$(\mathrm{S}): \quad \begin{cases} D_t^{q_1} x_s = a_1 x_s - a_2 y_s - a_2 z_s - d_3 w_s - a_1 x_s^2/M + \widetilde{s}_{w1}\Phi_1, \\ D_t^{q_2} y_s = b_3 N x_s - b_1 y_s - b_2 z_s - b_3 x_s (x_s - z_s) + \widetilde{s}_{w2}\Phi_2, \\ D_t^{q_3} z_s = -c_1 c_3 z_s + c_1 c_2 x_s z_s + \widetilde{s}_{w3}\Phi_3, \\ D_t^{q_4} w_s = d_1 x_s - d_2 w_s + \widetilde{s}_{w4}\Phi_4. \end{cases} \tag{52}$$

The initial conditions ensuring the chaotic behavior of (M) and (S) are (0.82, 0.29, 0.48, 0.1) and (0.78, 0.35, 0.4, 0.15), respectively, as considered in [63]. The chaotic attractors of the uncontrolled master and slave Fo-ERDS hyperchaotic systems are illustrated in Figure 3.

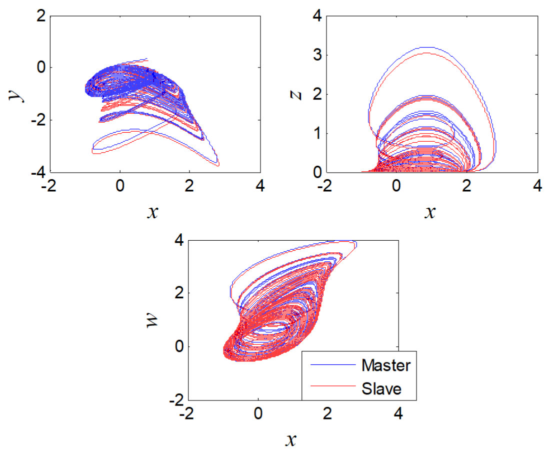

Figure 3: The chaotic attractors

The 'optimal' knowledge base of the F-oPD controller ensuring perfect synchronization is obtained after approximately 100 iterations: $\Lambda_{\mathrm{KB}} = \{(0.097, 0.066), (1, 0, 0, 0), 3, 0.98, 0.01\}$. When the F-oPD control signal is applied at $t \geqslant 6.34$ [sec] as for $\zeta = 0.01$, perfect synchronization is established in a limited period of time and the constraints related to the synchronization process given in Theorem 2 are established. Figure 4a illustrates that the tracking error between the state variables of the slave and those of the master systems are quickly returned to the original points, confirming that the master and the slave are perfectly synchronized. Figure 4b represents the corresponding input signal.

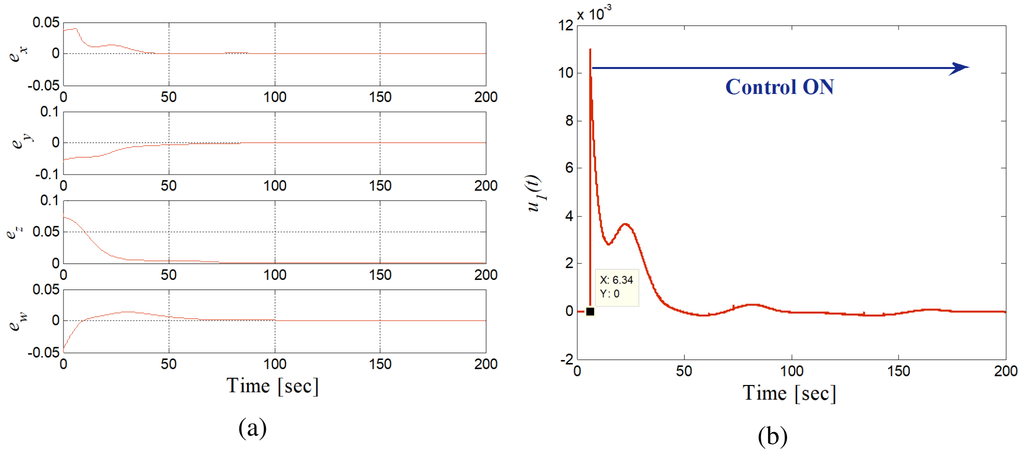

Figure 4: Tracking errors (a) and control input (b)

After conducting comparison simulations resembling the stabilization scenario, we find that the observations made regarding the stabilization process remain applicable when considering the synchronization case. Based on the comparison results, it can be inferred that the F-oPD control design approach exhibits superior performance compared to the integer-order control, despite utilizing the same optimization process. It is noteworthy that the proposed controller achieves convergence with relatively short transient responses. Furthermore, the tracking error quickly returns to its initial point, indicating the stability of the Fo-ERDS hyperchaotic system within a limited time frame.

Although considerable efforts have been devoted to approximating fractional operators and applying optimization techniques, the sizing of controller design and computation time are considered significant drawbacks during the modeling and simulation phase of functioning F-oCSs.

6. Conclusion

In this study, a F-oPD approach with a feasible knowledge base has been proposed. The stability evaluation is successfully conducted using both Lyapunov's direct method and the latest stability hypotheses for fractional-order dynamical systems. To meet the design criteria, we utilize the artificial hummingbird algorithm, a bio-inspired optimization technique inspired by the flight skills and foraging behavior of hummingbirds, to select the knowledge base of the F-oPD scheme. The design strategy proposed in this work offers significant benefits, including simplicity of implementation, reduced computation time, minimal data storage space, reduced energy consumption, high numerical precision, absence of oscillations, and guaranteed system stability. The results demonstrate improved performance in the stabilization and synchronization of the Fo-ERDS hyperchaotic system, validating the feasibility and effectiveness of the proposed approach.

References

[1] A.K. Jonscher: Dielectric relaxation in solids. *Journal of Physics D: Applied Physics*, **32**(14), (1999), 57–70. DOI: 10.1088/0022-3727/32/14/201.

[2] S. Westerlund and L. Ekstam: Capacitor Theory. *IEEE Transactions on Dielectrics and Electrical Insulation*, **1**(5), (1994), 826–839. DOI: 10.1109/94.326654.

[3] J.A. Tenreiro Machado and A.M.S.F. Galhano: Fractional order inductive phenomena based on the skin effect. *Nonlinear Dynamics*, **68**(1-2), (2012), 107–115. DOI: 10.1007/s11071-011-0207-z.

[4] I.S. Jesus and J.A. Tenreiro Machado: Development of fractional order capacitors based on electrolyte processes. *Nonlinear Dynamics*, **56**(1-2), (2009), 45–55. DOI: 10.1007/s11071-008-9377-8.

[5] I. Petráş: *Fractional-order nonlinear systems: Modeling, analysis and simulation*. Higher Education Press, Beijing and Springer-Verlag Berlin Heidelberg, 2011. DOI: 10.1007/978-3-642-18101-6.

[6] N. Bertrand, J. Sabatier, O. Briat and J. Vinassa: Fractional non-linear modelling of ultracapacitors. *Communications in Nonlinear Science and Numerical Simulation*, **15**(5), (2010), 1327–1337. DOI: 10.1016/j.cnsns.2009.05.066.

[7] S. Fang and X. Wang: Modeling and analysis method of fractional-order buck–boost converter. *International Journal of Circuit Theory and Applications*, **48**(9), (2020), 493–510. DOI: 10.1002/cta.2840.

[8] A.G. Radwan, A.A.Emira, A.M. AbdelAty and A.T. Azar: Modeling and analysis of fractional order DC-DC converter. *ISA Transactions*, **82** (2018), 184–199. DOI: 10.1016/j.isatra.2017.06.024.

[9] X. Chen, Y. Chen, B. Zhang and D. Qiu: A modeling and analysis method for fractional-order DC-DC converters. *IEEE Transactions on Power Electronics*, **32**(9), (2017), 7034–7044. DOI: 10.1109/TPEL.2016.2628783.

[10] Y. Ning-Ning, L. Chong-Xin and W. Chao-Jun: Modeling and dynamic analysis of the fractional-order Buck-Boost converter in continues conduction mode. *Chinese Physical Society*, **21**(8), (2012), 1–7. DOI: 10.1088/1674-1056/21/8/080503.

[11] F. Wang and X. Ma: Modeling and analysis of the fractional order buck converter in DCM operation by using fractional calculus and the circuit-averaging technique. *Journal of Power Electronics*, **13**(6), (2013), 1008–1015. DOI: 10.6113/JPE.2013.13.6.1008.

[12] A.M. Movahhed, H.T. Shandiz and S.K.H. Sani: Comparison of fractional order modelling and integer order modelling of fractional order buck converter in continuous condition mode operation. *Power Engineering and Electrical Engineering*, **14**(5), (2016), 531–542. DOI: 10.15598/aeee.v14i5.1635.

[13] W. Mitkowski, M. Długosz and P. Skruch: Selected engineering applications of fractional-order calculus. In: P. Kulczycki, J. Korbicz and J. Kacprzyk, (eds.), *Fractional Dynamical Systems: Methods, Algorithms and Applications. Studies in Systems, Decision and Control*, **402** Springer, Cham, 2022. DOI: 10.1007/978-3-030-89972-1_12.

[14] I. Podlubny: *Fractional differential equations*. New York: Academic Press, 1999.

[15] A. Oustaloup: *La Dérivation non entière*. Hermès, Paris 1991. In French.

[16] A. Soukkou, M.C. Belhour and S. Leulmi: Review, design, optimisation and stability analysis of fractional-order PID controller. *International Journal of Intelligent Systems and Applications*, **8**(7), (2016), 73–96. DOI: 10.5815/ijisa.2016.07.08.

[17] H. Zhu, S. Zhou and J. Zhang: Chaos and synchronization of the fractional-order Chua's system. *Chaos, Solitons and Fractals*, **39**(4), (2009), 1595–1603. DOI: 10.1016/j.chaos.2007.06.082.

[18] K. Diethelm, N.J. Ford and A.D. Freed: A predictor-corrector approach for the numerical solution of fractional differential equations. *Nonlinear Dynamics*, **29**(1), (2002), 3–22. DOI: 10.1023/A:1016592219341.

[19] E. Demirci and N. Ozalp: A method for solving differential equations of fractional order. *Journal of Computational and Applied Mathematics*, **236**(11), (2012), 2754–2762. DOI: 10.1016/j.cam.2012.01.005.

[20] L. Chen, W. Pan, K. Wang, R. Wu, J.A. Tenreiro Machado and A.M. Lopes: Generation of a family of fractional order hyper-chaotic multi-scroll attractors. *Chaos, Solitons & Fractals*, **105** (2017), 244–255. DOI: 10.1016/j.chaos.2017.10.032.

[21] T.C. Lin and T.Y. Lee: Chaos synchronization of uncertain fractional-order chaotic systems with time delay based on adaptive fuzzy sliding mode control. *IEEE Transactions on Fuzzy Systems*, **19**(4), (2011), 623–635. DOI: 10.1109/TFUZZ.2011.2127482.

[22] Z. Gao and X. Liao: Discretization algorithm for fractional order integral by Haar wavelet approximation. *Applied Mathematics and Computation*, **218**(5), (2011), 1917–1926. DOI: 10.1016/j.amc.2011.07.003.

[23] A.K. Mani and M.D. Narayanan: Analytical and numerical solution of ann-term fractional nonlinear dynamic oscillator. *Nonlinear Dynamics*, **100**, (2020), 999–1012. DOI: 10.1007/s11071-020-05539-0.

[24] A.H. Bukhari, M.A. Zahoor Raja, N. Rafiq, M. Shoaib, A.K. Kiani and Ch-M. Shu: Design of intelligent computing networks for nonlinear chaotic fractional Rossler system. *Chaos, Solitons and Fractals*, **157** (2022), 111985. DOI: 10.1016/j.chaos.2022.111985.

[25] Y. Wang, L. Zhu and Z. Wang: Fractional-order Euler functions for solving fractional integro-differential equations with weakly singular kernel. *Advances in Difference Equations*, **254** (2018), 1–13. DOI: 10.1186/s13662-018-1699-3.

[26] M.M. Khader: Generalized fractional-order Legendre polynomials and its treatment for solving system of FDEs. *Indian Journal of Physics*, **96** (2022), 3239–3246. DOI: 10.1007/s12648-021-02264-1.

[27] F.A. Shah and M. Irfan: Generalized wavelet method for solving non-steady heat transfer model of fractional order. *SeMA Journal*, **78** (2021), 541–556. DOI: 10.1007/s40324-021-00248-z.

[28] H. Hassani, J.A. Tenreiro Machado, E. Naraghirad and B. Sadeghi: Solving nonlinear systems of fractional-order partial differential equations using an optimization technique based on generalized polynomials. *Computational and Applied Mathematics*, **39**(300), (2020), 1–19. DOI: 10.1007/s40314-020-01362-w.

[29] W. Beghami, B. Maayah, S. Bushnaq and O. Abu Arqub: The Laplace optimized decomposition method for solving systems of partial differential

equations of fractional order. *International Journal of Applied and Computational Mathematics*, **8**(52), (2022), 1–18. DOI: 10.1007/s40819-022-01256-x.

[30] M.S. Tavazoei: Fractional order chaotic systems: history, achievements, applications, and future challenges. *European Physics Journal*, **229** (2020), 887–904. DOI: 10.1140/epjst/e2020-900238-8.

[31] M.A. Balootaki, H. Rahmani, H. Moeinkhah and A. Mohammadzadeh: On the synchronization and stabilization of fractional-order chaotic systems: Recent advances and future perspectives. *Physica A: Statistical Mechanics and its Applications*, **551**(2), (2020), 124203. DOI: 10.1016/j.physa.2020.124203.

[32] A. Oustaloup: *La Commande CRONE: Commande Robuste d'Ordre Non Entier*. Editions Hermès, Paris, 1991. In French.

[33] I. Podlubny: Fractional-order systems and $PI^{\lambda}D^{\mu}$ controllers. *IEEE Transactions on Automatic Control*, **44**(1), (1999), 208–214. DOI: 10.1109/9.739144.

[34] M.S. Tavazoei and M. Haeri: Chaotic attractors in incommensurate fractional order systems. *Physica D: Nonlinear Phenomena*, **237**(20), (2008), 2628–2637. DOI: 10.1016/j.physd.2008.03.037.

[35] X. Zhang, X. Zhang, D. Li and D. Yang: Adaptive synchronization for a class of fractional order time-delay uncertain chaotic systems via fuzzy fractional order neural network. *International Journal of Control, Automation and Systems*, **17**(5), (2019), 1209–1220. DOI: 10.1007/s12555-018-0342-0.

[36] A. Soukkou, A. Boukabou and S. Leulmi: Prediction-based feedback control and synchronization algorithm of fractional-order chaotic systems. *Nonlinear Dynamics*, **85**(4), (2016), 2183–2206. DOI: 10.1007/s11071-016-2823-0.

[37] A. Soukkou, A. Boukabou and S. Leulmi: Design and optimization of generalized prediction-based control scheme to stabilize and synchronize fractional-order hyperchaotic systems. *International Journal for Light and Electron Optics*, **127**(12), (2016), 5070–5077. DOI: 10.1016/j.ijleo.2016.02.044.

[38] A. Soukkou and S. Leulmi: Controlling and synchronizing of fractional-order chaotic systems via simple and optimal fractional-order feedback controller. *International Journal of Intelligent Systems and Applications*, **8**(6), (2016), 56–69. DOI: 10.5815/ijisa.2016.06.0.

[39] A. Soukkou and S. Leulmi: Elaboration of a generalized approach to control and to synchronize the fractional-order chaotic systems. *International Journal of General Systems*, **46**(8), (2017), 853–878. DOI: 10.1080/03081079.2017.1324854.

[40] A. Soukkou, A. Boukabou and A. Goutas: Generalized fractional-order time-delayed feedback control and synchronization designs for a class of fractional-order chaotic systems. *International Journal of General Systems*, **47**(7), (2018), 679–713. DOI: 10.1080/03081079.2018.1512601.

[41] S.M. Abedi Pahnehkolaei, A. Alfi and J.A. Tenreiro Machado: Fuzzy logic embedding of fractional order sliding mode and state feedback controllers for synchronization of uncertain fractional chaotic systems. *Computational and Applied Mathematics*, **39**(182), (2020), 1–16. DOI: 10.1007/s40314-020-01206-7.

[42] L.M. Martinez-Patiño, F.J. Perez-Pinal and A.G.S. Sánchez: Comparison between discretization techniques on HIL fractional-order controllers. *2022 IEEE Transportation Electrification Conference & Expo (ITEC)*, Anaheim, CA, USA, (2022), 467–472. DOI: 10.1109/ITEC53557.2022.9814049.

[43] J.C. Trigeassou and N. Maamri: *Analysis, modeling and stability of fractional order differential systems 1: The infinite state approach*. Wiley Publisher, August 2019.

[44] S. Huang and B. Wang: Stability and stabilization of a class of fractional-ordernonlinear systems for $0 < \alpha < 2$. *Nonlinear Dynamics*, **88** (2017), 973–984. DOI: 10.1007/s11071-016-3288-x.

[45] B.K. Lenka and S. Banerjee: Sufficient conditions for asymptotic stability and stabilization of autonomous fractional order systems. *Communications in Nonlinear Science and Numerical Simulation*, **56** (2018), 365–379. DOI: 10.1016/j.cnsns.2017.08.005.

[46] B.K. Lenka and S.N. Bora: New global asymptotic stability conditions for a class of nonlinear time-varying fractional systems. *European Journal of Control*, **63** (2022), 97–106. DOI: 10.1016/j.ejcon.2021.09.008.

[47] Z. Zhang, Y. Wang, J. Zhang, Z. Ai and F. Liu: Novel stability results of multivariable fractional-order system with time delay. *Chaos, Solitons and Fractals*, **157** (2022), 111943. DOI: 10.1016/j.chaos.2022.111943.

[48] V. K. Yadav, V.K. Shukla and S. Das: Exponential synchronization of fractional-order complex chaotic systems and its application. *Chaos, Solitons & Fractals*, **147** (2021), 110937. DOI: 10.1016/j.chaos.2021.110937.

[49] B. Zhang and X. Shu: *Fractional-order electrical circuit theory*. CPSS Power Electronics Series, 2022. DOI: 10.1007/978-981-16-2822-1.

[50] E. Tlelo-Cuautle, A.D. Pano-Azucena, O. Guillén-Fernández and A. Silva-Juárez: *Analog/Digital implementation of fractional order chaotic circuits and applications*. Springer Nature Switzerland AG, 2020. DOI: 10.1007/978-3-030-31250-3.

[51] J. Yao, K. Wang, P. Huang, L. Chen and J.A. Tenreiro Machado: Analysis and implementation of fractional-order chaotic system with standard components. *Journal of Advanced Research*, **25** (2020), 97–109. DOI: 10.1016/j.jare.2020.05.008.

[52] M.F. Tolba, H. Saleh, B. Mohammad, M. Al-Qutayri, A.S. Elwakil and A.G. Radwan: Enhanced FPGA realization of the fractional-order derivative and application to a variable-order chaotic system. *Nonlinear Dynamics*, **99** (2020), 3143–3154. DOI: 10.1007/s11071-019-05449-w.

[53] M. Wang: Dynamics, synchronization and circuit implementation of a simple fractional-order chaotic system with hidden attractors. *Chaos, Solitons & Fractals*, **130** (2020), 109406. DOI: 10.1016/j.chaos.2019.109406.

[54] Y. Wei, Q. Gao, Y. Chen and Y. Wang: Design and implementation of fractional differentiators, Part I: System based methods. *Control Engineering Practice*, **84** (2019), 297—304. DOI: 10.1016/j.conengprac.2018.12.008.

[55] A. Soukkou and A. Boukabou: Advanced Design of Fractional-order Controllers: Design and Optimization of Generalized PD-based Control Scheme to Stabilize and to Synchronize Fractional-order Hyperchaotic Systems. In *Advanced synchronization control and bifurcation of chaotic fractional-order systems*, IGI Global Publischer, Hershey PA, USA 17033, 2018, 305–332. DOI: 10.4018/978-1-5225-5418-9.ch011.

[56] M.A. Duarte-Mermoud, A. Aguila-Camacho, J.A. Gallegos and R. Castro-Linares: Using general quadratic Lyapunov functions to prove Lyapunov uniform stability for fractional order systems. *Communications in Nonlinear Science and Numerical Simulation*, **22**(1-3), (2015), 650–659. DOI: 10.1016/j.cnsns.2014.10.008.

[57] Y. Li, Y.Q. Chen and I. Podlubny: Stability of fractional-order nonlinear dynamic systems: Lyapunov direct method and generalized Mittag–Leffler stability. *Computers & Mathematics with Applications*, **59**(5), (2010), 1810–1821. DOI: 10.1016/j.camwa.2009.08.019.

[58] W. Zhao, L. Wang and S. Mirjalili: Artificial hummingbird algorithm: A new bio-inspired optimizer with its engineering applications. *Computer Methods in Applied Mechanics and Engineering*, **388** (2022), 1–13. DOI: 10.1016/j.cma.2021.114194.

[59] U.M. Diwekar: *Introduction to applied optimization*. Springer Cham, 2020. DOI: 10.1007/978-3-030-55404-0.

[60] M. Sun, L. Tian and Y. Fu: An energy resources demand–supply system and its dynamical analysis. *Chaos, Solitons & Fractals*, **32**(1), (2007), 168–180. DOI: 10.1016/j.chaos.2005.10.085.

[61] M. Sun, L. Tian and Y. Fu: A new four-dimensional energy resources system and its linear feedback control. *Chaos, Solitons & Fractals*, **39**(1), (2009), 101–108. DOI: 10.1016/j.chaos.2007.01.125.

[62] B. Xin, T. Chen and Y. Liu: Projective synchronization of chaotic fractional-order energy resources demand–supply systems via linear control. *Communications in Nonlinear Science and Numerical Simulation*, **16**(11), (2011), 4479–4486. DOI: 10.1016/j.cnsns.2011.01.021.

[63] S. Lavanya, C. Pradeep and S. Nagarani: Projective synchronization of fractional-order chaotic energy resource systems via linear control based on Takagi-Sugeno fuzzy model. *AIP Conference Proceedings*, **2261** (2020), 030127. DOI: 10.1063/5.0017268.